ACS NANO

www.acsnano.org

ARTICLE

Bioproduced Polymers Self-Assemble with Graphene Oxide into Nanocomposite Films with Enhanced Mechanical Performance

Kuang Liang,[#] Ewa M. Spiesz,[#] Dominik T. Schmieden, An-Wu Xu,* Anne S. Meyer,* and Marie-Eve Aubin-Tam*

Cite This: *ACS Nano* 2020, 14, 14731−14739

Read Online

ACCESS | Metrics & More | Article Recommendations | Supporting Information

ABSTRACT: Graphene oxide (GO) has recently been highlighted as a promising multipurpose two-dimensional material. However, free-standing graphene oxide films suffer from poor strength and flexibility, which limits scaling-up of production and lifetime structural robustness in applications. Inspired by the relationship between the organic and inorganic components of the hierarchical structure of nacre found in mollusk shells, we have fabricated self-assembled, layered graphene-based composite films. The organic phase of our composite is produced *via* environmentally friendly and economical methods based on bacterial production of γ-poly(glutamic acid) (PGA). Composite films made of GO, PGA, and divalent cations (Ca^{2+}) were prepared through a slow solvent evaporation method at ambient temperature, resulting in a nacre-like layered structure. These biobased nanocomposite films showed impressive mechanical properties, which resulted from a synergistic combination of hydrogen bonding with the bacterially produced PGA and ionic bonding with calcium ions (Ca^{2+}). The GO/PGA/Ca^{2+} composite films possessed a high strength of 150 ± 51.9 MPa and a high Young's modulus of 21.4 ± 8.7 GPa, which represents an increase of 120% and over 70% with respect to pure GO films. We provide rational design strategies for the production of graphene-based films with improved mechanical performance, which can be applied in filtration purification of wastewater in the paper, food, beverage, pigment, and pharmaceuticals industries, as well as for manufacturing of functional membranes and surface coatings.

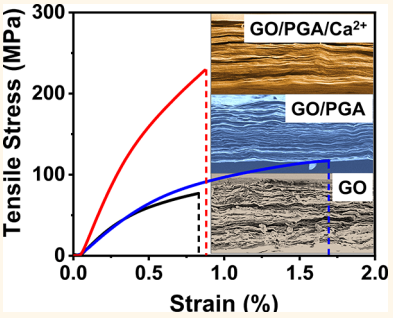

KEYWORDS: *composite film, graphene oxides, bacterial-produced γ-poly(glutamic acid), ionic bonding, mechanical properties*

Nacre, the layer lining the inside of many mollusk shells, exhibits high mechanical performance that combines remarkable toughness and tensile strength due to its unique "brick and mortar" layered structure. Natural nacre is a composite of brittle inorganic $CaCO_3$ and biological macromolecules (including β-chitin and silk fibroin-like proteins).[1] In recent years, a range of structural materials and synthetic methods have been successfully explored for the production of nacre-like hierarchical composites that show high stiffness without sacrificing toughness. While these two properties are often mutually exclusive, both are necessary for many load-bearing composite applications.[2−4] These techniques produced layer-by-layer (LBL) and/or self-assembled structures with excellent mechanical properties, exceeding those predicted by the rule of mixtures for composite material behavior. For example, more than 20 years ago, an efficient assembly process to fabricate an LBL structure was reported based on a simple dip-coating method, producing a silica/poly(dodecyl methacrylate) composite material.[5] Thereafter, a material closely replicating the mechanical strength of natural biocomposites was produced from clay−polyelectrolyte multilayers that approached the tensile strength of nacre.[6] More recently, Finnemore *et al.* and Spiesz *et al.* have both reported nacre-simulating materials composed of layer-by-layer structures of $CaCO_3$ and polymers.[7,8] These promising techniques have not yet been used for large-scale materials production due to constraints including complex processing,[7] rigorous fabrication conditions,[9] or costly waste treatment.[10] Despite the active development of nacre-inspired materials, it still remains a challenge to identify practical routes of producing robust nacre-like materials for wide usage and large-scale applications.

Graphene oxide (GO) is an advantageous material for fabricating nacre-inspired composites due to its natural ability

Received: February 2, 2020
Accepted: October 28, 2020
Published: November 4, 2020

https://dx.doi.org/10.1021/acsnano.0c00913
ACS Nano 2020, 14, 14731−14739

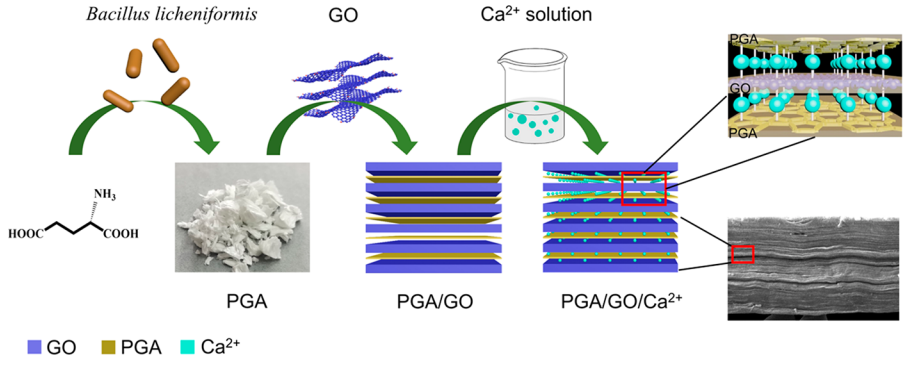

Figure 1. Schematic illustration of the preparation process for GO/PGA/Ca^{2+} composite films.

to self-assemble into ordered and layered structures.[11] Graphene is a two-dimensional (2D) and single-atom-thick material consisting of a lattice of sp^2-bonded carbon, which has attracted interest in areas including biosensing,[12] catalysis,[13] electrochemistry,[14] energy,[15] and decontamination.[16] Graphene oxide, the oxidized state of graphene, not only possesses excellent mechanical strength,[17] but the various functional groups anchored on the edges of GO sheets make them beneficial for the preparation of carbon-based functional materials.[18,19] GO films are often applied as water purification membranes, but their life span, and therefore cost-efficiency, is limited by the membrane robustness.[20] Free-standing graphene oxide films suffer from poor strength, toughness, and flexibility that limit their use because GO sheets typically form networks only *via* weak van der Waals forces.[21] Therefore, the preparation of graphene oxide films with robust mechanical performance has not yet been accomplished. Several polymers have been suggested to improve the mechanical properties of GO films.[5,22,23] However, these previous studies use chemically produced polymers, which are costly and generate toxic waste. In our study, we report a GO-based material that is mechanically improved through the use of a bacterially produced polymer, which is environmentally friendly and cost-effective.

One promising strategy to improve the mechanical properties of GO films is to introduce a polymer with appropriate functional groups that can form bridges between GO sheets, such as poly(acrylic acid), carboxyl methyl cellulose, or chitosan.[24−27] In this work, we apply a bacterially produced polymer that shows potential as a candidate to strengthen GO films: γ-poly(glutamic acid) acid (PGA). PGA exhibits numerous useful physicochemical and biological properties because of its nontoxicity, hydrophilicity, and biodegradability.[28,29] Interestingly, PGA is a naturally occurring polymer and can be easily and efficiently produced by bacteria in large amounts, and thanks to its economic and environmentally friendly nature, PGA has found versatile applications.[30] In contrast to other environmentally friendly polymers, PGA can be easily and efficiently produced in large scale by bacteria, providing an economic and sustainable nature that has allowed PGA to be useful in versatile applications. Since PGA contains multiple functional groups (including −COOH and $-NH_2$), it can interact with surface-modified GO nanosheets, making them more electronegative and hydrophilic *via* electrostatic forces and polar effects.[31] Our biological manufacturing approach is unique to the field of GO-based composites production and will guide advanced, sustainable directions to prepare bioinspired nacre-mimetic materials.

In this work, we show that PGA polymers and GO nanosheets will self-assemble with each other into thin films that are robust and mechanically stable. To further improve the mechanical properties of GO films, we combined GO, PGA, and Ca^{2+} ions for the preparation of nacre-inspired multilayered composite films. Incorporation of metal ions such as Ca^{2+} or Zn^{2+} into the internal structure of GO-based films is proposed to form ionic bonds with the negatively charged functional groups on the PGA polymers, leading to significant improvement of the mechanical properties and higher stability of nacre-like composite materials.[32,33] Characterization of our GO/PGA/Ca^{2+} films indicated that the introduction of PGA and Ca^{2+} significantly enhanced the mechanical properties of the GO films due to synergistic interface interactions of hydrogen bonding with PGA and ionic bonding with Ca^{2+}, resulting in a reinforced nacre-like multilayered structure. The tensile strength of the bioinspired films exhibited high ultimate stress (150 ± 51.9 MPa) and an outstanding Young's modulus (21.4 ± 8.7 GPa), which represents a 120% and 70% increase with respect to pure GO films. Our approach for fabricating a self-assembled layered composite is a low-effort and inexpensive process for preparing large-scale, highly ordered multilayer films with industrial applications such as filtration of wastewater, functional membranes,[20] fabrics,[34] or coatings.[35]

RESULTS AND DISCUSSION

In order to produce a mechanically robust, nacre-inspired biobased material *via* a rapid, practical method, we developed a technique for producing self-assembled, layered materials based on cross-linked GO thin films. First, γ-poly(glutamic acid) polymer was produced with *Bacillus licheniformis* bacteria. Next, GO/PGA hybrid films were prepared by mixing an aqueous suspension solution of GO and PGA, in which PGA molecules adsorbed onto exfoliated GO nanosheets *via* hydrogen bonding.[36] GO/PGA/Ca^{2+} films were then obtained by immersing the GO/PGA films into a calcium chloride solution (Figure 1). Our hypothesis was that the Ca^{2+} ions would interlink the PGA polymer chains and the GO nanosheets *via* complexing with their oxygen-containing functional groups, which in turn would improve the mechanical properties of the GO-based composites.

To determine the influence of PGA on the mechanical properties of Ca^{2+}-linked GO/PGA nanocomposite films and optimize the PGA content for best mechanical performance, we prepared ternary nanocomposites of GO/PGA/Ca^{2+} with varying mass fractions of GO and PGA, including GO:PGA ratios of 100:0, 100:3 100:5, 100:8, and 100:10. Tensile strength testing of these materials showed that the GO/PGA/

https://dx.doi.org/10.1021/acsnano.0c00913
ACS Nano 2020, 14, 14731−14739

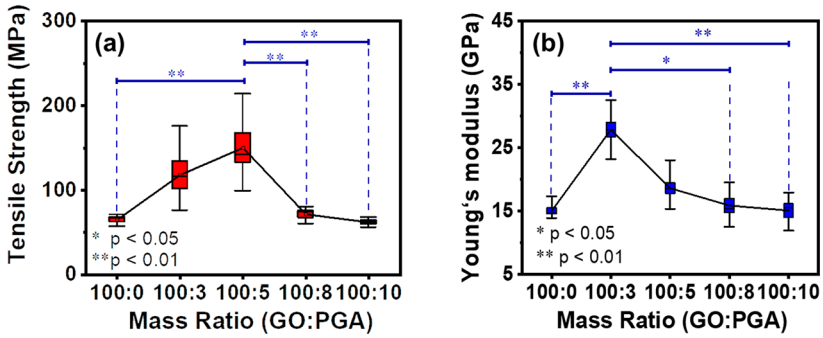

Figure 2. Mechanical properties of GO/PGA/Ca^{2+} nanocomposites containing different ratios of GO to PGA: 100:0 (no PGA), 100:3; 100:5; 100:8, and 100:10. (a) Tensile strength and (b) Young's modulus of the nanocomposites. GO/PGA/Ca^{2+} composite films with a GO:PGA ratio of 100:5 possessed the highest tensile strength of 150.1 ± 51.9 MPa. The nanocomposite film with a GO:PGA ratio of 100:3 achieved the highest Young's modulus of 27.8 ± 3.8 GPa. * represents significant differences with a *p*-value of <0.05, and ** represents significant differences with a *p*-value of <0.01. The GO:PGA ratio of 100:5 was chosen for all subsequent experiments.

Ca^{2+} composite film with a GO:PGA ratio of 100:5 possessed the highest tensile strength of 150.1 ± 51.9 MPa (Figure 2a). This trend is consistent with toughness properties of our materials; the GO/PGA/Ca^{2+} composite film with a GO:PGA ratio of 100:5 reached a toughness of 1.32 ± 0.34 (MJ m^{-3}), superior to the films with other ratios (Figure S1). The nanocomposite film with a GO:PGA ratio of 100:3 achieved the highest Young's modulus of 27.8 ± 3.8 GPa (Figure 2b), which is far higher than other graphene-based composite films reported in the literature.[37−39] Materials with GO:PGA ratios of 100:3 and 100:5 were significantly stronger and stiffer than all other tested ratios ($p < 0.05$, Figure 2); their strength and stiffness were not significantly different from each other ($p > 0.05$). The significant improvement of tensile strength and stiffness upon the addition of intermediate amounts of PGA is likely related to generation of additional ionic bonds formed with Ca^{2+}, while higher amounts of polymer are detrimental to tensile strength and stiffness, as observed in GO:PVA composites.[24] We chose the GO:PGA ratio of 100:5 for all subsequent experiments, therefore the general names "GO:PGA" and "GO/PGA/Ca^{2+} composite films" refer to 100:5 GO:PGA ratios throughout the rest of this work.

The morphologies of cross sections of GO, GO/Ca^{2+}, GO/PGA, and GO/PGA/Ca^{2+} composite films were examined with scanning electron microscopy (SEM) to assess the effect of PGA and/or Ca^{2+} on the structure of the GO-based films. The pure GO films (Figure 3a) exhibited a wavy layered structure with abundant interlayer gaps, which were likely caused by weak hydrogen-bonding interactions between adjacent GO nanosheets. Upon introducing either PGA or Ca^{2+} ions, the gaps between the GO nanolayers appeared to decrease (Figure 3b−d), suggesting improved interfacial interactions due to the polymer or metal ions. Compared with pure GO or GO/PGA, the amount of space within GO/Ca^{+} films or GO/PGA/Ca^{2+} film was further decreased, and the layers were stacked closer together (details of the interlayer space quantification are shown in Table S1 and Figure S2), indicating that a stronger integration occurred within the film. The samples containing calcium ions (GO/Ca^{2+} and GO/PGA/Ca^{2+}) contained layers that appeared flatter and more densely packed after the treatment with Ca^{2+}. The insertion of calcium ions thus seemed to successfully lead to the formation of ionic bonds between Ca^{2+} and the carboxyl groups in GO and/or PGA.

The stacked layers visible by SEM imaging represent GO assemblies, each of which is made up of many GO nanosheets.

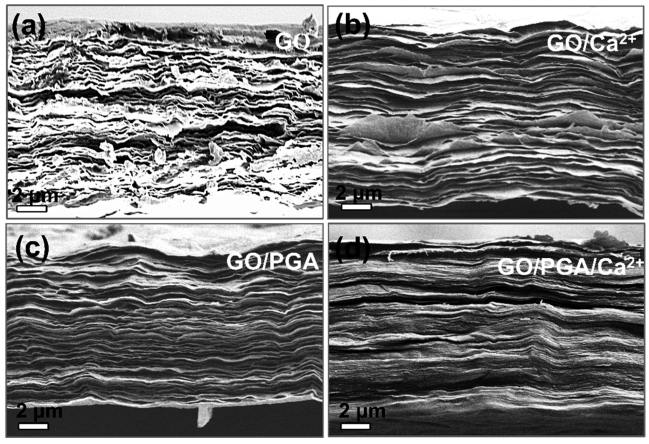

Figure 3. SEM images of the cross sections of nacre-inspired films: (a) GO, (b) GO/Ca^{2+}, (c) GO/PGA, and (d) GO/PGA/Ca^{2+} films. The layered structures became increasingly dense after treatment with Ca^{2+} solution.

To investigate the morphological changes in the density of the nanosheet stacking in our GO materials, X-ray diffraction (XRD) was employed for crystallographic and structural analysis of the GO, GO/PGA, and GO/PGA/Ca^{2+} layered materials (Figure 4a). A strong peak was observed in the XRD pattern for each sample at approximately 10.8°, which is characteristic of GO.[40] The position of this peak was used to determine the interlayer distance (*d*-spacing) of the GO nanosheet layers according to Bragg's law. The introduction of PGA or PGA together with calcium ions caused the GO peak to shift toward smaller angles, indicating larger spacing of GO nanosheet layers. The *d*-spacing of the pure GO film was determined to be 0.82 nm, which increased to 0.84 nm for the GO/PGA composite, indicating that the PGA molecules were successfully intercalated into the GO nanosheets. The *d*-spacing value further increased to 0.89 nm after treatment with calcium ions to produce GO/PGA/Ca^{2+}, which is evidence that Ca^{2+} was also successfully introduced into the interlayers of GO/PGA. The presence of Ca^{2+} ions within the GO layers was directly verified by energy dispersive X-ray spectrometry (EDS) analysis (Figure S3). Our composite materials thus display hierarchical internal structuring, whereby the introduction of PGA and Ca^{2+} swells the thickness of each lower-order GO nanosheet but results in closer packing of higher-order GO assemblies. The added PGA and Ca^{2+} is likely bound

https://dx.doi.org/10.1021/acsnano.0c00913
ACS Nano 2020, 14, 14731−14739

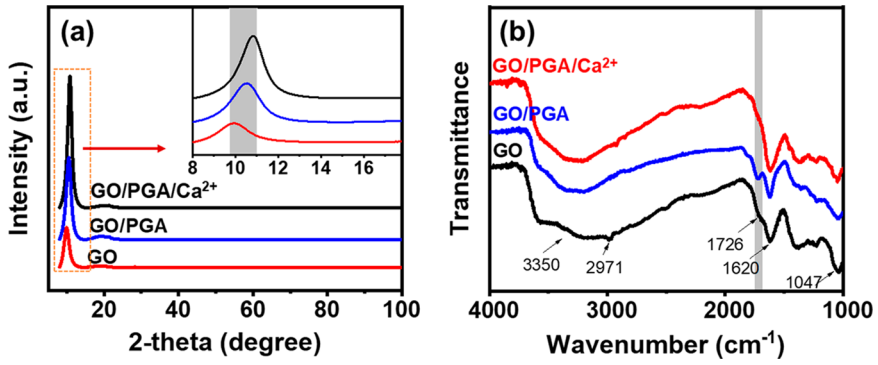

Figure 4. (a) XRD patterns of the GO (black), GO/PGA (blue), and GO/PGA/Ca^{2+} (red) composite films. The inset displays a magnified view of the XRD peak at 10.8°, characteristic of GO. The shift of this peak reflects changing *d*-spacing values, indicating the insertion of PGA molecules and Ca^{2+} ions into the GO nanolayers. (b) FTIR analysis of GO (black), GO/PGA (blue), and GO/PGA/Ca^{2+} (red) films. The peak at 1726 cm^{-1} corresponding to C═O stretching vibration indicates the generation of hydrogen bonds between PGA and GO in the GO/PGA films.

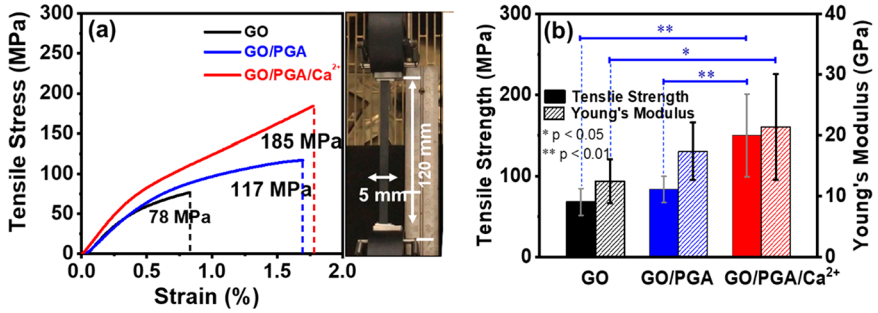

Figure 5. (a) Representative stress−strain curves of GO, GO/PGA, and GO/PGA/Ca^{2+} composite films from uniaxial tensile tests. The right image shows the grips used in the tests. The maximal tensile strength obtained for a given film type is indicated next to the curve. (b) Tensile strength and Young's modulus properties of GO (black), GO/PGA (blue), and GO/PGA/Ca^{2+} (red) films. Data are shown as mean with standard deviation. * represents significant differences with a *p*-value of <0.05, and ** represents significant differences with a *p*-value of <0.01.

not only between nanosheets but also between assemblies of nanosheets, resulting in additional reinforcement.

The interfacial interactions among GO, PGA, and Ca^{2+} components were analyzed using Fourier transform infrared (FTIR) spectroscopy (Figure 4b), X-ray photoelectron spectroscopy (XPS) (Figure S4), and Raman spectroscopy (Figure S5). The FTIR curve of GO displayed a strong −OH peak at 3350 cm^{-1}, C−H asymmetric stretching at 2971 cm^{-1}, C═C bonds at 1620 cm^{-1}, C═O bonds at 1726 cm^{-1}, and C−O−C bonds at 1047 cm^{-1}.[41,42] Similar peaks were observed in GO/PGA and GO/PGA/Ca^{2+}. Interestingly, the peak of the C═O stretching vibration band in carboxyl groups was enhanced after the introduction of PGA, implying that PGA molecules were hydrogen-bonded onto the GO sheets. That peak was diminished after the introduction of Ca^{2+} ions, which can be explained by complexation between Ca^{2+} and GO carboxylic groups causing an increased spacing between GO nanosheets (Figure 4b) that weakened hydrogen-bonding interactions.[43,44] Next, from XPS spectroscopy, the C 1s spectra (Figure S4a−c) revealed that the addition of PGA into the GO film resulted in a significant decrease of the C−O−C component (287.0 eV) and an increase of the C−OH component (285.9 eV), which could be caused by the ring-opening reaction of epoxides, which generates alcohol groups.[45] Meanwhile, the percentage of oxygen-containing functional groups dramatically decreased in GO/PGA/Ca^{2+}, suggesting chemical cross-linking with Ca^{2+} ions (Figure S4d). In addition, a slight shift of the O 1s peak from 532.5 eV in GO to 532.3 eV in GO/PGA and GO/PGA/Ca^{2+} samples and a massive decrease in intensity of the O 1s peak after treatment in the Ca^{2+} solution could be ascribed to the linkage occurring between Ca^{2+}, PGA, and GO. Furthermore, in the Raman spectra (Figure S5), the intensity ratios of I_D/I_G for GO, GO/PGA, and GO/PGA/Ca^{2+} were found to be 0.941, 0.951 and 0.959, respectively. This increase in I_D/I_G value upon addition of PGA and Ca^{2+} is due to an increase in the number of sp^2 domains, further confirming interaction between the components in the composite film.[46]

The mechanical performance of our GO-based layered materials was evaluated through tensile testing (Table S2). Typical stress−strain curves of GO, GO/PGA, and GO/PGA/Ca^{2+} films are shown in Figure 5a. The tensile strength of pure GO films was 68.2 ± 16.6 MPa, and the Young's modulus was 12.5 ± 3.6 GPa (Figure 5b), consistent with previous reports.[45] After incorporating bacteria-derived PGA, the modified GO/PGA film exhibited a tensile strength of 83.7 ± 16.3 MPa (22.7% increase compared to pure GO, $p = 0.63$) and a Young's modulus of 17.4 ± 4.8 GPa (39.2% increase compared to pure GO, $p = 0.28$). Only after incorporating Ca^{2+} ions into the composite did the Young's modulus increase significantly to 21.4 ± 8.7 GPa ($p < 0.05$, see Figure 4), and the tensile strength was dramatically increased to 150.1 ± 51.9 MPa ($p < 0.01$), which is comparable to natural nacre (tensile strength of 170 MPa)[9] and 120% higher than pure GO.

https://dx.doi.org/10.1021/acsnano.0c00913
ACS Nano 2020, 14, 14731−14739

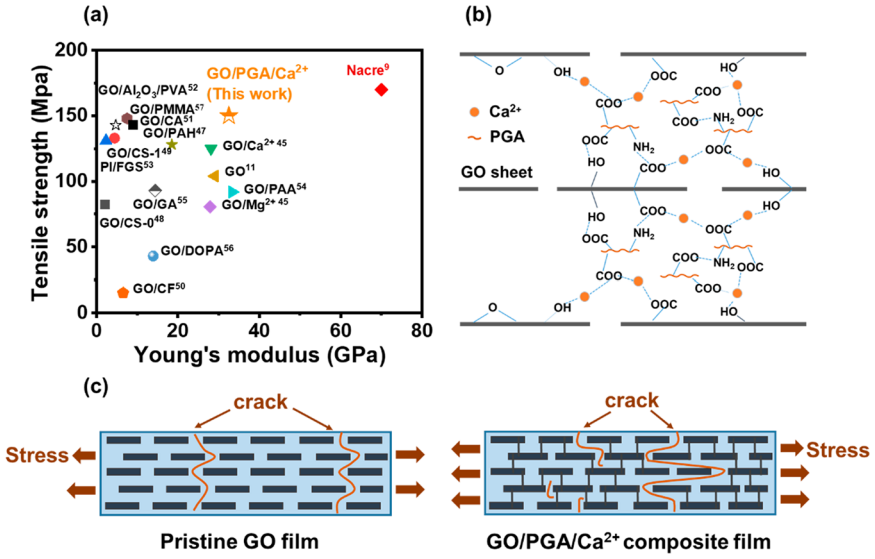

Figure 6. (a) Comparison of the mechanical properties of the layered GO/PGA/Ca^{2+} nanocomposites with natural nacre and other GO-based films: GO,[11] GO/PAH,[47] GO/CS,[48,49] GO/CF,[50] GO/CA,[51] GO/Al_2O_3/PVA,[52] GO/FGS,[53] GO/Mg^{2+},[45] GO/PAA,[54] GO/GA,[55] GO/Ca^{2+},[45] GO/DOPA,[56] and GO/PMMA.[57] Our bioinspired GO/PGA/Ca^{2+} nanocomposites show greatly improved mechanical properties compared to other GO-based films. See Figure S6 for a comparison of tensile strength *versus* toughness. (b) Schematic illustrations of the synergistic interactions of hydrogen bond cross-linking and ionic bonds established between GO, PGA, and Ca^{2+} in our composite material and (c) the fracture mechanisms proposed for the pristine GO and GO/PGA/Ca^{2+} composite films.

The synergistic effect of adding both intermolecular hydrogen and ionic bonding together in the same material provides our bioinspired nanocomposites with mechanical properties that approximate natural nacre and are superior to those of other GO-based nanocomposites (Figure 6a). For example, GO/poly(allylamine) hydrochloride (PAH)[47] shows a tensile strength of 128.22 ± 19.15 MPa, but its Young's modulus is only 18.31 ± 1.27 GPa. A lower stiffness is also observed in GO/chitosan (CS),[48,49] GO/carbon fiber (CF),[50] GO/CA,[51] GO/Al_2O_3/PVA,[52] and polyimide/functionalized graphene (PI/FGS).[53] The tensile strength of our GO/PGA/Ca^{2+} is more than 1.6 times higher than that of GO/poly allylamine (PAA)[54] and GO/glutaraldehyde (GA).[55] While the Young's modulus of our material is close to that of GO/Ca^{2+} (28.1 ± 1.2 GPa) and GO/Mg^{2+} (27.9 ± 1.8 GPa),[45] which are also cross-linked *via* ionic bonds, the tensile strength of these materials is significantly lower than in our PGA-containing materials. Compared with GO/dopamine (DOPA) composites,[56] the tensile strength and stiffness of the GO/PGA/Ca^{2+} nanocomposite are 6.5 and 2.3 times higher, respectively. The tensile strength of the GO/PGA/Ca^{2+} nanocomposite is comparable to GO/hydrophobic poly-(methyl methacrylate) (PMMA) (148 MPa),[57] and the stiffness is 4.3 times higher than that (7.5 GPa). Overall, our GO/PGA/Ca^{2+} composite exhibits a combination of high strength and excellent stiffness, outperforming other GO-based films.

The high mechanical performance of our self-assembled, nacre-inspired GO/PGA/Ca^{2+} composite films can be attributed to several factors. First, the solvent evaporation self-assembly of graphene oxide sheets led to the formation of two-dimensional, highly ordered layered nacre-like films. This structure, with abundant gaps between the layers, acted as a matrix that could be filled by PGA polymer and Ca^{2+} ions, thus improving the mechanical performance of the nanocomposite films. Next, the XRD results (Figure 4a) demonstrated that PGA molecules were well-intercalated within the GO films. The abundant oxygen-containing functional groups on both GO and PGA provided the basis for the formation of hydrogen bonds, which increased the tensile strength of the films. Finally, Ca^{2+} is reported to have a strong ability to chelate with anionic polymers[58] and was thus likely able to interlink the PGA polymer chains within the GO nanosheets *via* complexing with these oxygen-containing functional groups. As a result, we conclude that our materials formed a cross-linked structure with strong intercalations between PGA, GO, and Ca^{2+} ions (Figure 6b). These modifications to GO films resulted in substantially improved mechanical performance in terms of both strength and stiffness, enabling various potential applications that require robust materials without losing the benefits inherent to GO-based materials such as their low cost and light weight.

We propose a possible fracture mechanism for the pristine GO and GO/PGA/Ca^{2+} composite films (Figure 6c). When tensile stress is applied to the films, adjacent sheets can slip relative to one another, resulting in the formation of cracks and leading to failure under high strains. Owing to the weak interactions between the adjacent sheets, GO sheets in non-cross-linked GO films are easily pulled out; hence, the pristine GO film exhibits a comparatively rough fracture edge.[55,59] After Ca^{2+} and PGA cross-linking, the enhanced interlayer interactions ensure only moderate sheet slippage, resulting in a smooth fracture edge of the GO/PGA/Ca^{2+} film. Our structurally stabilized, cross-linked GO/PGA/Ca^{2+} composite structure may help overcome the challenge of the instability of the interlayer spacing between adjacent GO nanosheets, which currently prevents the usage of GO membranes as separation barriers.[60]

Stability in different environments, such as high-temperature or moist conditions, is an important aspect for evaluating the suitability of a material for specific applications. We conducted thermogravimetric analysis (TGA) to reveal the thermal stability of the composite films. The GO/PGA/Ca^{2+} samples started to decompose when the temperature rose above 200

https://dx.doi.org/10.1021/acsnano.0c00913
ACS Nano 2020, 14, 14731−14739

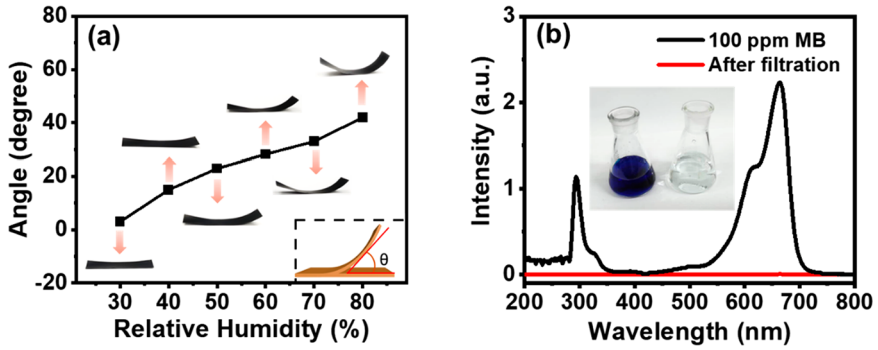

Figure 7. (a) Bending angle of the GO/PGA/Ca^{2+} composite film measured at different relative humidity (RH) values. The inset shows a schematic depiction of the bending angle. (b) Ultraviolet−visible spectra of the MB solution (100 ppm, black) and the filtrate (red); the inset image shows the MB solution (100 ppm) before filtration (left) and the filtrate (right).

°C, indicating that the composite film remains thermally stable up to 200 °C (Figure S7). Also, the GO/PGA and GO/PGA/Ca^{2+} composite films showed good stability and remained intact when immersed in water for 25 days, while pure GO films showed poor tolerance to water and fractured into pieces (Figure S8). Additionally, the response of the GO/PGA/Ca^{2+} composite film to humidity was tested to demonstrate its structural stability when exposed to humid environments. Upon increasing the relative humidity from 30% to 80%, the composite became increasingly bent, reaching an angle of only 42.7° at 80% relative humidity. This result demonstrates excellent shape stability (Figure 7a). Moreover, the hydrophilicity of the GO/PGA/Ca^{2+} composite film was characterized by a sessile drop experiment. A contact angle of 37.1 ± 2.8° was obtained for a drop of water on the surface of the composite film, showing high hydrophilicity (Figure S9).[61] Furthermore, we used the GO/PGA/Ca^{2+} composite film to filter an organic dye commonly present in wastewater from dye-related industries. Methyl blue (MB), a dye commonly used in the textile industry, could be filtered through our GO/PGA/Ca^{2+} film with over 99% filtering efficiency (Figure 7b).

CONCLUSIONS

Composite films of PGA and graphene oxide were successfully prepared and mechanically reinforced with Ca^{2+} ions. The GO/PGA/Ca^{2+} nanocomposites can be fabricated using a simple, low cost, easily scaled-up, and environmentally friendly method using water as the processing solvent. The obtained GO/PGA/Ca^{2+} composite films have a nacre-like layered structure, achieving greatly enhanced mechanical performance. The cross-linking of GO with bacteria-produced PGA polymer in the presence of Ca^{2+} improved the mechanical properties of the composites as compared to unmodified GO films. The maximum tensile strength and Young's modulus values of the GO/PGA/Ca^{2+} composite films measured here reached up to 150.1 ± 51.9 MPa and 21.4 ± 8.7 GPa, respectively, which are similar to natural nacre in terms of strength and stiffness. The excellent mechanical performance and environmental stability of our composite films make them promising for applications in water purification (*e.g.*, drinking water purification, waste treatment, food and beverage industry applications), functional membrane manufacturing (for membrane-based separation technologies), surface coatings, and other industries that require low-cost raw materials, simple synthesis technology, energy-efficiency, easy scale-up, and environmental friendliness, all combined with excellent mechanical properties.

METHODS

Materials. All chemical reagents used in this work were obtained from VWR Netherlands.

PGA was produced with bacteria (*Bacillus licheniformis*) using a microorganism-induced method, as explained in detail previously.[8] Briefly, *B. licheniformis* (NBRC12107, NBRC, Japan) was grown in medium E (20 g/L L-glutamic acid, 13.6 g/L monosodium citrate, 80 g/L glycerol, 7 g/L NH_4Cl, 0.5 g/L KH_2PO_4, 0.244 g/L $MgSO_4$, 0.04 g/L $FeCl_3{\cdot}6H_2O$, 0.15 g/L $CaCl_2{\cdot}2H_2O$, 0.1 g/L $MnSO_4{\cdot}H_2O$, pH 7.5 with NaOH, sterilized by autoclaving).[62] PGA was isolated from the growth medium by adding $CuSO_4$ to a concentration of 0.4 M. The precipitated PGA was isolated by centrifugation (30000*g* for 30 min) and redissolved in 0.5 M ethylenediaminetetraacetic acid (EDTA) solution. Cu-EDTA complexes were removed by dialysis against water, after which the PGA was lyophilized (Christ Alpha 1-2 LD Plus lyophilizer) and stored dry at room temperature until use.

Graphene oxide nanosheets were synthesized from natural graphite powder according to a modified Hummer and Offeman method.[63] Briefly, 1.5 g of natural graphite flakes was added to a mixture of concentrated H_2SO_4 (97%) and H_3PO_4(85%) (180 mL:20 mL) in a conical flask. Nine grams of well-ground $KMnO_4$ powder was slowly added to the mixture while the temperature was maintained at 35 °C in a water bath. The reaction was then heated to 50 °C and stirred for 12 h. When the reaction had completed, the mixture was poured into 200 mL of water chilled by ice, followed by immediate addition of H_2O_2 (5 mL). The product was obtained by centrifugation at 3000 rpm for 5 min and washed with 5% HCl solution to remove the remaining metal ions, then washed with deionized water (DI). Finally, the dense GO solution was lyophilized.

Preparation of GO/PGA/Ca^{2+} Composite Film. GO/PGA films were prepared by a spontaneous mixing method. To prepare a GO dispersion, prepared GO was diluted with DI water to a concentration of 5 g/L and sonicated for 5 h, then centrifuged at 4000 rpm for 30 min to remove the unreacted graphite and multilayered graphene oxide. The supernatant was collected and dialyzed for a week in DI water that was exchanged daily. Next, various amounts of PGA were dissolved in the GO dispersion in a 240W Emmi-D30 sonication bath. Films with different weight ratios of GO to PGA (100:3, 100:5, 100:8, and 100:10) were prepared and evaluated to determine an optimal ratio for mechanical performance. The mixture was transferred to a Petri dish, and composite films were formed by drying for 4 days at room temperature. The prepared films were cut by a razor blade into strips with a width of 5 mm and a length of approximately 150 mm (a format required for mechanical testing, according to ASTM standard D-882-02) before further treatment (Figure S10a). GO/PGA/Ca^{2+} composite films were prepared by immersing the precut GO/PGA strips in a 0.5 M $CaCl_2$ solution overnight at room temperature. The strips were removed from solution, washed with DI water three times, and finally dried in air at room temperature (Figure S10b).

Structural and Mechanical Characterization. Films were characterized by SEM with EDS, XRD, FTIR, and uniaxial tension

https://dx.doi.org/10.1021/acsnano.0c00913
ACS Nano 2020, 14, 14731−14739

tests. For SEM analysis, samples were spin-coated with an 8 nm layer of gold and imaged with a Nova NanoSEM under 5−15 kV voltage. XPS analysis was conducted using a PerkinElmer RBD upgraded PHI-5000C ESCA system. The Raman spectrum was collected on a Raman microscope (Renishaw) with a 514.5 nm excitation source operating on a LabRAM HR Evolution Raman microscope. Quantitative analyses of the cross sections of composite samples were performed to measure the change in thickness before and after Ca^{2+} treatment with the same batch of GO or GO/PGA films using ImageJ software. At least 10 sites were analyzed in SEM images of the same magnification to measure average thickness of the films and calculate the associated interlayer spacing. To calculate interlayer distances and determine crystal polymorphs, XRD patterns of the films were recorded on a Bruker D8 Advance diffractometer with Cu Kα radiation (λ = 1.541 78 Å), with the operation voltage and current set at 40 kV and 40 mA, respectively. Film samples were ground into fine powder before performing XPS using a PerkinElmer RBD upgraded PHI-5000C ESCA system. Mechanical properties were measured on an Instron tester with a gauge length of 100 mm, according to ASTM standard D-882-02. Sample width was 5 mm. The testing rate was 2 mm/min, and samples that broke in the vicinity of the grips (within 10 mm, or 10% of full specimen length) were excluded. At least five samples per condition were tested to ensure reproducibility.

The response behaviors of the composite film to moisture were tested in a sealed transparent box equipped with a hygrometer, and a humidistat was applied to record and monitor the relative humidity. The hydrophilicity of the GO/PGA/Ca^{2+} composite film was assessed with a sessile drop experiment by depositing a 5.7 μL droplet of water onto a GO/PGA/Ca^{2+} film, and the contact angle of the drop was measured five times to calculate the average value using a contact angle goniometer (INNUO CA100D). Methyl blue was chosen as an example to visualize the efficiency of our composite's filtering capabilities. A vacuum filtration system equipped with our GO/PGA/Ca^{2+} composite film as the filter was built (Figure S11) and used to filter an MB solution with a concentration of 100 ppm in water. After filtering, the filtering efficiency was determined with an ultraviolet−visible spectrophotometer.

Statistics. Statistical analyses were performed with Gnumeric software (v. 1.10.16). Sample normality was tested using Anderson−Darling tests and qq plots. Normally distributed samples are presented as means ± standard deviations. Samples for which normality could not be ensured are presented as medians ± interquartile range. Samples were compared using one-way (single factor) ANOVA tests and *posthoc* Tukey's HSD (honest significant difference) tests, with a significance level of α = 0.05.

ASSOCIATED CONTENT

Supporting Information

The Supporting Information is available free of charge at https://pubs.acs.org/doi/10.1021/acsnano.0c00913.

Additional figures and tables: thickness of GO/Ca^{2+} and GO/PGA/Ca^{2+} films, toughness of GO/PGA/Ca^{2+} nanocomposites containing different ratios of GO to PGA, representative EDS image of GO/PGA/Ca^{2+} film, summary of the films' mechanical properties, XPS and Raman curves of GO, GO/PGA, and GO/PGA/Ca^{2+} films, comparison of the mechanical properties of GO/PGA/Ca^{2+} nanocomposites with natural nacre and other GO-based films, TGA of GO, GO/PGA, and GO/PGA/Ca^{2+} films, stability of GO, GO/PGA, and GO/PGA/Ca^{2+} films immersed in water for 25 days, digital photos of water drops on GO/PGA/Ca^{2+} composite film, images of filtration setup, pictures of fabricated films (PDF)

AUTHOR INFORMATION

Corresponding Authors

An-Wu Xu − *Division of Nanomaterials and Chemistry, Hefei National Laboratory for Physical Sciences at Microscale, University of Science and Technology of China, Hefei 230026, Anhui, China;* orcid.org/0000-0002-4950-0490; Phone: +86-551-63602346; Email: anwuxu@ustc.edu.cn

Anne S. Meyer − *Department of Biology, University of Rochester, Rochester, New York 14620, United States;* Email: anne.meyer@rochester.edu

Marie-Eve Aubin-Tam − *Department of Bionanoscience, Delft University of Technology, 2629 HZ Delft, The Netherlands;* orcid.org/0000-0001-9995-2623; Email: M.E.Aubin-Tam@tudelft.nl

Authors

Kuang Liang − *Department of Bionanoscience, Delft University of Technology, 2629 HZ Delft, The Netherlands; Division of Nanomaterials and Chemistry, Hefei National Laboratory for Physical Sciences at Microscale, University of Science and Technology of China, Hefei 230026, Anhui, China*

Ewa M. Spiesz − *Department of Bionanoscience, Delft University of Technology, 2629 HZ Delft, The Netherlands*

Dominik T. Schmieden − *Department of Bionanoscience, Delft University of Technology, 2629 HZ Delft, The Netherlands*

Complete contact information is available at: https://pubs.acs.org/10.1021/acsnano.0c00913

Author Contributions

#K. Liang and E. M. Spiesz contributed equally to this work.

Notes

The authors declare no competing financial interest.

ACKNOWLEDGMENTS

The authors gratefully acknowledge funding support from the National Natural Science Foundation of China (grant nos. 51572253, 21771171), a Scientific Research Grant of Hefei National Synchrotron Radiation Laboratory (grant no. UN2017LHJJ), and the Fundamental Research Funds for the Central Universities (grant no. YD2340002001). This work was primarily conducted at Delft University of Technology and was supported by The Netherlands Organization for Scientific Research (NWO/OCW), as part of the Advanced Materials NWO-NSFC program (grant no. 729.001.016) and the China Scholarship Council (CSC) that provided the financial support during the visit of K. Liang to Delft University of Technology. R. Kieffer is acknowledged for support with the experimental setup, and R. Hendrikx is acknowledged for assisting with the XRD analyses.

REFERENCES

(1) Corni, I.; Harvey, T. J.; Wharton, J. A.; Stokes, K. R.; Walsh, F. C.; Wood, R. J. K. A Review of Experimental Techniques to Produce a Nacre-Like Structure. *Bioinspiration Biomimetics* **2012**, *7*, 031001.

(2) Gao, H.; Chen, S.; Mao, L.; Song, Z. Q.; Yao, H. B.; Cölfen, H.; Luo, X. S.; Zhang, F.; Pan, Z.; Meng, Y. F.; Ni, Y.; Yu, S. H. Mass Production of Bulk Artificial Nacre with Excellent Mechanical Properties. *Nat. Commun.* **2017**, *8*, 287.

(3) Wang, Y.; Mei, Y. F.; Huang, Y. X.; Li, Y.; Li, J.; Meng, F.; Zhou, Z. Ultra-Robust and High-Toughness Graphene Oxide Papers *via* Synergistic Strengthening by Addition of Carbon-Nanotubes and Copper Ions. *Carbon* **2019**, *147*, 490−500.

(4) Gao, Y.; Xu, H.; Cheng, Q. Multiple Synergistic Toughening Graphene Nanocomposites through Cadmium Ions and Cellulose Nanocrystals. *Adv. Mater. Interfaces* **2018**, *5*, 1800145.
(5) Sellinger, A.; Weiss, P. M.; Nguyen, A.; Lu, Y.; Assink, R. A.; Gong, W.; Brinker, C. J. Continuous Self-Assembly of Organic-Inorganic Nanocomposite Coatings that Mimic Nacre. *Nature* **1998**, *394*, 256−260.
(6) Tang, Z.; Kotov, N. A.; Magonov, S.; Ozturk, B. Nanostructured Artificial Nacre. *Nat. Mater.* **2003**, *2*, 413−418.
(7) Finnemore, A.; Cunha, P.; Shean, T.; Vignolini, S.; Guldin, S.; Oyen, M.; Steiner, U. Biomimetic Layer-By-Layer Assembly of Artificial Nacre. *Nat. Commun.* **2012**, *3*, 966−971.
(8) Spiesz, E. M.; Schmieden, D. T.; Grande, A. M.; Liang, K.; Schwiedrzik, J.; Filipe, N. F.; Michler, J.; Garcia, S. J.; Aubin-Tam, M. E.; Meyer, A. S. Bacterially-Produced, Nacre-Inspired Composite Materials. *Small* **2019**, *15*, 1805312.
(9) Georgakilas, V.; Tiwari, J. N.; Kemp, K. C.; Perman, J. A.; Bourlinos, A. B.; Kim, K. S.; Zboril, R. Noncovalent Functionalization of Graphene and Graphene Oxide for Energy Materials, Biosensing, Catalytic, and Biomedical Applications. *Chem. Rev.* **2016**, *116*, 5464−5519.
(10) Walther, A.; Bjurhager, I.; Malho, J. M.; Ruokolainen, J.; Berglund, L.; Ikkala, O. Supramolecular Control of Stiffness and Strength in Lightweight High-Performance Nacre-Mimetic Paper with Fire-Shielding Properties. *Angew. Chem., Int. Ed.* **2010**, *49*, 6448−6453.
(11) Dikin, D. A.; Stankovich, S.; Zimney, E. J.; Piner, R. D.; Dommett, G. H. B.; Evmenenko, G.; Nguyen, S. T.; Ruoff, R. S. Preparation and Characterization of Graphene Oxide Paper. *Nature* **2007**, *448*, 457−460.
(12) Park, J.; Kim, B.; Han, J.; Oh, J.; Park, S.; Ryu, S.; Jung, S.; Shin, J.; Lee, B. S.; Hong, B. H.; Choi, D.; Kim, B. S. Graphene Oxide Flakes as a Cellular Adhesive: Prevention of Reactive Oxygen Species Mediated Death of Implanted Cells for Cardiac Repair. *ACS Nano* **2015**, *9*, 4987−4999.
(13) Hou, Y.; Wen, Z.; Cui, S.; Ci, S.; Mao, S.; Chen, J. An Advanced Nitrogen-Doped Graphene/Cobalt-Embedded Porous Carbon Polyhedron Hybrid for Efficient Catalysis of Oxygen Reduction and Water Splitting. *Adv. Funct. Mater.* **2015**, *25*, 872−882.
(14) Lehner, B. A.; Janssen, V. A.; Spiesz, E. M.; Benz, D.; Brouns, S. J.; Meyer, A. S.; van der Zant, H. S. Creation of Conductive Graphene Materials by Bacterial Reduction Using Shewanella Oneidensis. *ChemistryOpen* **2019**, *8*, 888−895.
(15) Zhou, G.; Li, L.; Ma, C.; Wang, S.; Shi, Y.; Koratkar, N.; Ren, W.; Li, F.; Cheng, H. A Graphene Foam Electrode with High Sulfur Loading for Flexible and High Energy Li-S Batteries. *Nano Energy* **2015**, *11*, 356−365.
(16) Perreault, F.; Faria, A. F.; Elimelech, M. Environmental Applications of Graphene-Based Nanomaterials. *Chem. Soc. Rev.* **2015**, *44*, 5861−5896.
(17) Liu, L.; Zhang, J.; Zhao, J.; Liu, F. Mechanical Properties of Graphene Oxides. *Nanoscale* **2012**, *4*, 5910−5916.
(18) Kim, J.; Cote, L. J.; Kim, F.; Yuan, W.; Shull, K. R.; Huang, J. Graphene Oxide Sheets at Interfaces. *J. Am. Chem. Soc.* **2010**, *132*, 8180−8186.
(19) Xing, W.; Yuan, B.; Wang, X.; Hu, Y. Enhanced Mechanical Properties, Water Stability and Repeatable Shape Recovery Behavior of Ca^{2+} Crosslinking Graphene Oxide-Based Nacre-Mimicking Hybrid Film. *Mater. Des.* **2017**, *115*, 46−51.
(20) Han, Y.; Xu, Z.; Gao, C. Ultrathin Graphene Nanofiltration Membrane for Water Purification. *Adv. Funct. Mater.* **2013**, *23*, 3693−3700.
(21) Liu, F.; Seo, T. S. A Controllable Self-Assembly Method for Large-Scale Synthesis of Graphene Sponges and Free-Standing Graphene Films. *Adv. Funct. Mater.* **2010**, *20*, 1930−1936.
(22) Tian, Y.; Cao, Y.; Wang, Y.; Yang, W.; Feng, J. Realizing Ultrahigh Modulus and High Strength of Macroscopic Graphene Oxide Papers through Crosslinking of Mussel-Inspired Polymers. *Adv. Mater.* **2013**, *25*, 2980−2983.
(23) Shin, M. K.; Lee, B.; Kim, S. H.; Lee, J. A.; Spinks, G. M.; Gambhir, S.; Wallace, G. G.; Kozlov, M. E.; Baughman, R. H.; Kim, S. J. Synergistic Toughening of Composite Fibres by Self-Alignment of Reduced Graphene Oxide and Carbon Nanotubes. *Nat. Commun.* **2012**, *3*, 650.
(24) Gong, S.; Cui, W.; Zhang, Q.; Cao, A.; Jiang, L.; Cheng, Q. Integrated Ternary Bioinspired Nanocomposites *via* Synergistic Toughening of Reduced Graphene Oxide and Double-Walled Carbon Nanotubes. *ACS Nano* **2015**, *9*, 11568−11573.
(25) Ha, H.; Shanmuganathan, K.; Ellison, C. J. Mechanically Stable Thermally Crosslinked Poly(acrylic Acid)/Reduced Graphene Oxide Aerogels. *ACS Appl. Mater. Interfaces* **2015**, *7*, 6220−6229.
(26) Yan, N.; Capezzuto, F.; Lavorgna, M.; Buonocore, G. G.; Tescione, F.; Xia, H.; Ambrosio, L. Borate Cross-Linked Graphene Oxide-Chitosan as Robust and High Gas Barrier Films. *Nanoscale* **2016**, *8*, 10783−10791.
(27) Gong, S.; Zhang, Q.; Wang, R.; Jianga, L.; Cheng, Q. Synergistically Toughening Nacre-Like Graphene Nanocomposites *via* Gel-Film Transformation. *J. Mater. Chem. A* **2017**, *5*, 16386−16392.
(28) Chen, P.; Qiu, M.; Deng, C.; Meng, F.; Zhang, J.; Cheng, R.; Zhong, Z. pH-Responsive Chimaeric Pepsomes Based on Asymmetric Poly(ethylene Glycol)-b-Poly(l-leucine)-b-Poly(l-glutamic acid) Triblock Copolymer for Efficient Loading and Active Intracellular Delivery of Doxorubicin Hydrochloride. *Biomacromolecules* **2015**, *16*, 1322−1330.
(29) Zhang, K.; Yan, S.; Li, G.; Cui, L.; Yin, J. *in Situ* Birth of MSCs Multicellular Spheroids in Poly(l-glutamic acid)/Chitosan Scaffold for Hyaline-Like Cartilage Regeneration. *Biomaterials* **2015**, *71*, 24−34.
(30) Schmieden, D. T.; Meyer, A. S.; Aubin-Tam, M. Using Bacteria to Make Improved, Nacre-Inspired Materials. *MRS Adv.* **2016**, *150*, 559−564.
(31) Kim, H. W.; Yoon, H. W.; Yoon, S.; Yoo, B. M.; Ahn, B. K.; Cho, Y. H.; Shin, H. J.; Yang, H.; Paik, U.; Kwon, S.; Choi, J. Y.; Park, H. B. Selective Gas Transport through Few-Layered Graphene and Graphene Oxide Membranes. *Science* **2013**, *342*, 91−96.
(32) Zhang, Z.; Zhu, J.; Han, Q.; Cui, H.; Bi, H.; Wang, X. Enhanced Photo-Electrochemical Performances of Graphene-Based Composite Functionalized by Zn^{2+} Tetraphenylporphyrin. *Appl. Surf. Sci.* **2014**, *321*, 404−411.
(33) Chen, K.; Tang, X.; Yue, Y.; Zhao, H.; Guo, L. Strong and Tough Layered Nanocomposites with Buried Interfaces. *ACS Nano* **2016**, *10*, 4816−4827.
(34) Cai, G.; Yang, M.; Xu, Z.; Liu, J.; Tang, B.; Wang, X. Flexible and Wearable Strain Sensing Fabrics. *Chem. Eng. J.* **2017**, *325*, 396−403.
(35) Gao, X.; Chen, L.; Ji, L.; Liu, X.; Li, H.; Zhou, H.; Chen, J. Humidity-Sensitive Macroscopic Lubrication Behavior of an As-Sprayed Graphene Oxide Coating. *Carbon* **2018**, *140*, 124−30.
(36) Liang, J.; Huang, Y.; Zhang, L.; Wang, Y.; Ma, Y.; Guo, T.; Chen, Y. Molecular-Level Dispersion of Graphene into Poly(vinyl Alcohol) and Effective Reinforcement of Their Nanocomposites. *Adv. Funct. Mater.* **2009**, *19*, 2297−2302.
(37) Gan, S.; Zakaria, S.; Jaafar, S. N. S. Enhanced Mechanical Properties of Hydrothermal Carbamated Cellulose Nanocomposite Film Reinforced with Graphene Oxide. *Carbohydr. Polym.* **2017**, *172*, 284−293.
(38) Kabiri, R.; Namazi, H. Nanocrystalline Cellulose Acetate (NCCA)/Graphene Oxide (GO) Nanocomposites with Enhanced Mechanical Properties and Barrier against Water Vapor. *Cellulose* **2014**, *21*, 3527−3539.
(39) Chen, M.; Yin, J.; Jin, R.; Yao, L.; Su, B.; Lei, Q. Dielectric and Mechanical Properties and Thermal Stability of Polyimide-Graphene Oxide Composite Films. *Thin Solid Films* **2015**, *584*, 232−237.
(40) Alam, S. N.; Sharma, N.; Kumar, L. Synthesis of Graphene Oxide (GO) by Modified Hummers Method and Its Thermal Reduction to Obtain Reduced Graphene Oxide (rGO). *Graphene* **2017**, *6*, 1−18.

https://dx.doi.org/10.1021/acsnano.0c00913
ACS Nano 2020, 14, 14731−14739

(41) Han, D.; Yan, L.; Chen, W.; Li, W. Preparation of Chitosan/Graphene Oxide Composite Film with Enhanced Mechanical Strength in the Wet State. *Carbohydr. Polym.* **2011**, *83*, 653−658.
(42) Wang, Y.; Yuan, H.; Ma, P.; Bai, H.; Chen, M.; Dong, W.; Xie, Y.; Deshmukh, Y. S. Superior Performance of Artificial Nacre Based on Graphene Oxide Nanosheets. *ACS Appl. Mater. Interfaces* **2017**, *9*, 4215−4222.
(43) Zhang, Y.; Li, Y.; Ming, P.; Zhang, Q.; Liu, T.; Jiang, L.; Cheng, Q. Ultrastrong Bioinspired Graphene-Based Fibers *via* Synergistic Toughening. *Adv. Mater.* **2016**, *28*, 2834−2839.
(44) Liang, B.; Zhao, H.; Zhang, Q.; Fan, Y.; Yue, Y.; Yin, P.; Guo, L. Ca^{2+} Enhanced Nacre-inspired Montmorillonite-Alginate Film with Superior Mechanical, Transparent, Fire Retardancy, and Shape Memory Properties. *ACS Appl. Mater. Interfaces* **2016**, *8*, 28816−28823.
(45) Park, S.; Lee, K. S.; Bozoklu, G.; Cai, W.; Nguyen, S. T.; Ruoff, R. S. Graphene Oxide Papers Modified by Divalent Ions—Enhancing Mechanical Properties *via* Chemical Cross-Linking. *ACS Nano* **2008**, *2*, 572−578.
(46) Shahzadi, K.; Mohsin, I.; Wu, L.; Ge, X.; Jiang, Y.; Li, H.; Mu, X. Bio-Based Artificial Nacre with Excellent Mechanical and Barrier Properties Realized by a Facile *in Situ* Reduction and Cross-Linking Reaction. *ACS Nano* **2017**, *11*, 325−334.
(47) Satti, A.; Larpent, P.; Gun'ko, Y. Improvement of Mechanical Properties of Graphene Oxide/Poly (allylamine) Composites by Chemical Crosslinking. *Carbon* **2010**, *48*, 3376−3381.
(48) Zuo, P. P.; Feng, H. F.; Xu, Z. Z.; Zhang, L. F.; Zhang, Y. L.; Xia, W.; Zhang, W. Q. Fabrication of Biocompatible and Mechanically Reinforced Graphene Oxide-Chitosan Nanocomposite Films. *Chem. Cent. J.* **2013**, *7*, 39.
(49) Pan, Y.; Wu, T.; Bao, H.; Li, L. Green Fabrication of Chitosan Films Reinforced with Parallel Aligned Graphene Oxide. *Carbohydr. Polym.* **2011**, *83*, 1908−1915.
(50) Kong, Q. Q.; Liu, Z.; Gao, J. G.; Chen, C. M.; Zhang, Q.; Zhou, G.; Tao, Z. C.; Zhang, X. H.; Wang, M. Z.; Li, F.; Cai, R. Hierarchical Graphene−Carbon Fiber Composite Paper as a Flexible Lateral Heat Spreader. *Adv. Funct. Mater.* **2014**, *24*, 4222−4228.
(51) Woo, J. Y.; Oh, J. H.; Jo, S.; Han, C. S. Nacre-Mimetic Graphene Oxide/Cross-Linking Agent Composite Films with Superior Mechanical Properties. *ACS Nano* **2019**, *13*, 4522−4529.
(52) Wang, J.; Qiao, J.; Wang, J.; Zhu, Y.; Jiang, L. Bioinspired Hierarchical Alumina−Graphene Oxide−Poly (vinyl Alcohol) Artificial Nacre with Optimized Strength and Toughness. *ACS Appl. Mater. Interfaces* **2015**, *7*, 9281−9286.
(53) Luong, N. D.; Hippi, U.; Korhonen, J. T.; Soininen, A. J.; Ruokolainen, J.; Johansson, L.; Nam, J.; Sinh, L. H.; Seppälä, J. Enhanced Mechanical and Electrical Properties of Polyimide Film by Graphene Sheets *via in Situ* Polymerization. *Polymer* **2011**, *52*, 5237−5242.
(54) Park, S.; Nguyen, S. T.; Ruoff, R. S. Graphene Oxide Sheets Chemically Cross-Linked by Polyallylamine. *J. Phys. Chem. C* **2009**, *113*, 15801−15804.
(55) Gao, Y.; Liu, L. Q.; Zu, S. Z.; Peng, K.; Zhou, D.; Han, B. H.; Zhang, Z. The Effect of Interlayer Adhesion on the Mechanical Behaviors of Macroscopic Graphene Oxide Papers. *ACS Nano* **2011**, *5*, 2134−2141.
(56) Zhong, D.; Yang, Q.; Guo, L.; Dou, S.; Liu, K.; Jiang, L. Fusion of Nacre, Mussel, and Lotus Leaf: Bio-Inspired Graphene Composite Paper with Multifunctional Integration. *Nanoscale* **2013**, *5*, 5758−5764.
(57) Putz, K. W.; Compton, O. C.; Palmeri, M. J.; Nguyen, S. T.; Brinson, L. C. High-Nanofiller-Content Graphene Oxide-Polymer Nanocomposites *via* Vacuum-Assisted Self-Assembly. *Adv. Funct. Mater.* **2010**, *20*, 3322−3329.
(58) Ji, D.; Choi, S.; Kim, J. A Hydrogel-Film Casting to Fabricate Platelet-Reinforced Polymer Composite Films Exhibiting Superior Mechanical Properties. *Small* **2018**, *14*, 1801042.
(59) Compton, O. C.; Cranford, S. W.; Putz, K. W.; An, Z.; Brinson, L. C.; Buehler, M. J.; Nguyen, S. T. Tuning the Mechanical Properties of Graphene Oxide Paper and Its Associated Polymer Nanocomposites by Controlling Cooperative Intersheet Hydrogen Bonding. *ACS Nano* **2012**, *6*, 2008−2019.
(60) Ma, J.; Ping, D.; Dong, X. Recent Developments of Graphene Oxide-Based Membranes: A Review. *Membranes* **2017**, *7*, 52.
(61) Wang, L.; Wang, Y.; Dai, J.; Tian, S.; Xie, A.; Dai, X.; Pan, J. Coordination-Driven Interfacial Cross-Linked Graphene Oxide-Alginate Nacre Mesh with Underwater Superoleophobicity for Oil-Water Separation. *Carbohydr. Polym.* **2021**, *251*, 117097.
(62) Kedia, G.; Hill, D.; Hill, R.; Radecka, I. Production of Poly-γ-Glutamic Acid by *Bacillus subtilis* and *Bacillus licheniformis* with Different Growth Media. *J. Nanosci. Nanotechnol.* **2010**, *10*, 5926−5934.
(63) Marcano, D. C.; Kosynkin, D. V.; Berlin, J. M.; Sinitskii, A.; Sun, Z.; Slesarev, A.; Alemany, L. B.; Lu, W.; Tour, J. M. Improved Synthesis of Graphene Oxide. *ACS Nano* **2010**, *4*, 4806−4814.

https://dx.doi.org/10.1021/acsnano.0c00913
ACS Nano 2020, 14, 14731−14739